

polymer review

New developments in polymer surface analysis

D. Briggs

ICI PLC, Petrochemicals and Plastics Division, PO Box 90, Wilton, Middlesbrough, Cleveland, TS6 8JE, UK

(Received 18 November 1983; revised 16 February 1984)

Surface and interface characterization of polymeric materials has not enjoyed the multi-technique approach which typifies other types of materials. X-ray photoelectron spectroscopy (XPS) has dominated, despite several major disadvantages. New approaches are discussed which either improve XPS (particularly derivatization techniques) or utilize 'static' secondary ion mass spectrometry (SIMS) to overcome these limitations, with examples of their application in materials problem solving.

(Keywords: polymer; surface; X-ray photoelectron spectroscopy; secondary ion mass spectrometry; derivatization; imaging)

INTRODUCTION

Compared with other classes of materials, organic polymeric systems are rather uniquely placed in the story of applied surface and interface characterization. This uniqueness derives from the combination of the two properties: very low electrical conductivities (10^{-13} – $10^{-18} \Omega^{-1} \text{ m}^{-1}$) and very high damage cross-sections under charged particle bombardment. Consequently, whilst the whole range of available surface and interface analysis techniques (principally XPS, AES, SIMS and *in situ* sputter depth-profiling) has been applied to materials problem solving involving metals/alloys, semi-conductors, ceramics and even glasses, the only technique easily applicable to polymeric materials has been XPS.

The potential of XPS for polymer surface investigation was recognized fairly early in the development of the technique¹ and there is no denying the contribution which XPS has made to problem solving in the polymeric materials field during the last decade^{2,3}. To those working in the polymer technology field, however, the limitations of XPS have been increasingly exposed with time. These are:

(1) Small dynamic range of core level chemical shifts and ambiguity of binding energies (e.g. of functionalities involving O and N).

(2) Very poor spatial resolution and lack of imaging.

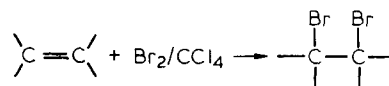
(3) Limited surface sensitivity, particularly when angular variation is impossible or inappropriate.

The principal object of this paper is to review recent work specifically aimed at overcoming these deficiencies, with examples to illustrate why XPS analysis alone is inadequate and how the new approaches either complement or supplant XPS to provide the required information. This work falls into two distinct categories. Firstly, the technique of derivatization, or functional group labelling, which aims to overcome limitation (1) above by providing a means to monitor quantitatively specific polymer surface functional groups. Secondly, the development of static SIMS for polymer surface analysis. Besides

providing fingerprint spectra of organic entities to complement conventional XPS data, SIMS has the inherent surface sensitivity to overcome limitation (3). It also has the potential for overcoming limitation (2) through the use of a scanning fine-focus beam. This review also considers other developments in XPS which, although of general utility, are important in this area.

POLYMER SURFACE DERIVATIZATION

Recognition that peaks with a particular BE in the XP spectra of polymers could correspond to more than one type of functional group was appreciated in the very early days of polymer surface modification studies³. Brecht *et al.*⁴ and Dwight and Riggs⁵ in independent XPS studies of PTFE etching by sodium solutions sought a means of quantifying unsaturation produced by the treatment, knowing that groups involving C–C or C–H bonds all have the same C_{1s} BE. Both teams hit on the idea of reacting the surface with bromine hoping that a selective reaction:



would take place, allowing the intensity of the Br signal which appeared in the spectrum to be used for quantification of the original number of unsaturated groups. This procedure is the first example of the derivative technique—the use of a reagent which reacts selectively with a particular functional group of interest, and in so doing introduces into the surface a 'label' or 'tag' atom easily recognised in the XP spectrum and capable of quantification. During the last few years, and correlating clearly with the more widespread use of XPS in detailed studies of processes and problems in the field of polymer technology, several groups have been forced into derivatization procedures through the realization that the basic XPS information is inadequate for complex polymer surface structural analysis.

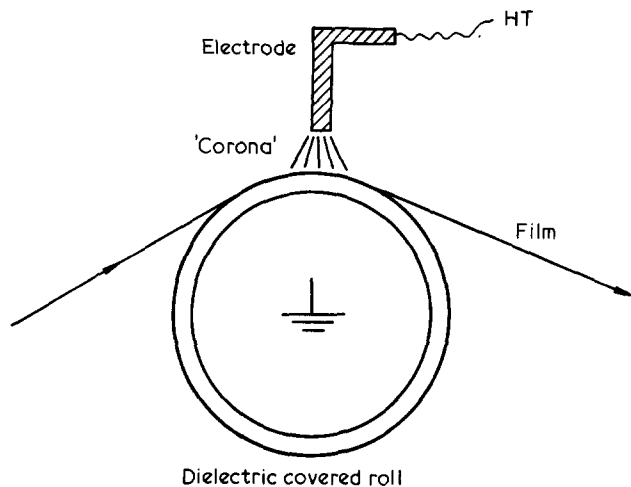


Figure 1 Schematic of electrical 'corona' discharge treatment process

This work has led to a growing body of literature on derivatization techniques and on the problems inherent in these experiments⁶⁻¹². The derivatization reaction should ideally proceed to completion within the total XPS sampling depth, quickly and under mild conditions. A gas phase reagent may satisfy these criteria but generally a solution phase reagent must be used. Reactions which proceed rapidly at room temperature in solution are often sterically hindered in the polymer surfaces layers. Solvents which permeate into the polymer are likely to aid reaction but may, at the same time, give rise to surface reorganization e.g. functional group migration into the bulk. These effects have recently been studied in detail by Everhart and Reilley⁹. Solvents may also extract lower molecular weight material produced during the surface modification process. The removal of unreacted reagent by washing can be particularly problematical if ionic derivatives are employed. Solvent-type reactions are thus generally a compromise between achieving complete derivatization and avoiding solvent-induced artefacts. Most of the work reported to date has concerned the investigation of polymer film surfaces and this has meant that angular variation experiments have been possible to check the vertical homogeneity of derivatized surfaces. Several compilations of derivatization reactions, particularly for oxygen functionalities, have appeared^{2,7,12} and the most detailed specific overview of the subject is by Reilley *et al.*¹². The difficulties of derivatization experiments are, therefore, not to be under-estimated, but the rewards are substantial as the following case history from the author's laboratory may illustrate.

The need to use derivatization procedures arose during a fundamental study of the electrical ('corona') discharge treatment process used to enhance the adhesive characteristics of polyolefin films (e.g. polyethylene and polypropylene). These hydrocarbon materials with low surface energies (31 mN m^{-2}) have inherently poor wettability and require a pretreatment before operations such as printing, adhesive bonding/lamination or coating can be successfully carried out. The pretreatments used all significantly raise the film surface energy although whether this alone is the reason for improved adhesion has been a very controversial subject for many years. A systematic study by XPS of commercially applied and other pretreatments by Briggs and co-workers¹³ underlined the importance of surface oxidation in all cases.

The particular case of corona discharge treatment is depicted schematically in Figure 1. The polymer film passes over an earthed metal roller covered with a dielectric (insulating) material. Separated from the film by $\sim 2 \text{ mm}$ is an electrode bar to which a high voltage is applied (typically 15 kV at 20 KHz). Air in the film electrode gap is ionized, the corona discharge thus formed is stable and this 'treats' the film surface. Prior to our studies other workers had carried out measurements on small scale set-ups, often using low frequency discharges, involving treatment in oxidizing and inert atmospheres. Adhesion enhancement was noted in all cases and this, together with reflection-i.r. spectroscopic data (sampling depth $\sim 1 \mu\text{m}$) led to the conclusion that surface chemical change was unimportant and that surface electret formation was the basis of adhesion improvement. On the other hand Owens at Du Pont, working only with an industrial unit and using indirect analytical methods, proposed¹⁴ that oxygen functionalities capable of H-bonding, introduced during treatment, were important in adhesion enhancement (this work is discussed in detail in refs. 13 and 15). A popular model system for adhesion studies has been the autoadhesion of low density polyethylene (LDPE) when two films are contacted under pressure. Untreated surfaces do not adhere when contacted below $\sim 90^\circ\text{C}$ but after corona discharge treatment autoadhesion can be obtained at a significantly lower temperature ($\sim 70^\circ\text{C}$). This is the so-called autoadhesion enhancement effect. The level of autoadhesion is measured by a peel test. Some of our data^{15,16} for LDPE treated in air, nitrogen and argon atmospheres in a small scale system are shown in Figure 2. In all cases the final surface contains oxygen and the autoadhesion (peel strength) corresponds well with surface oxygen concen-

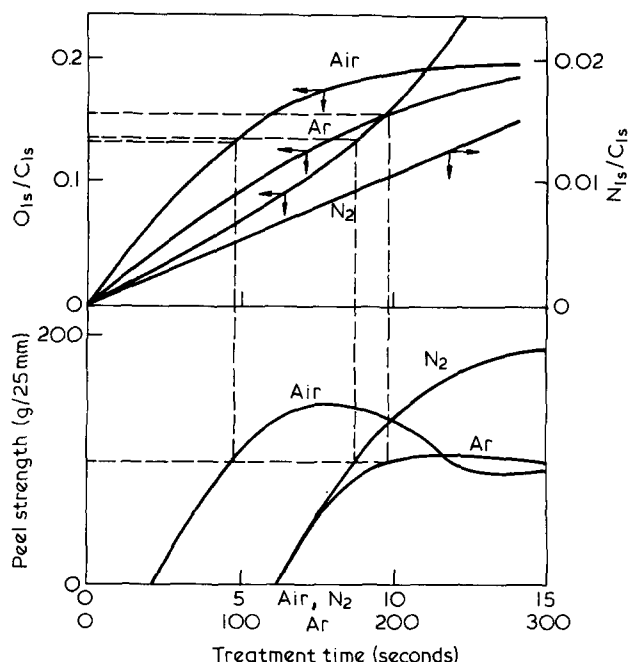


Figure 2 Comparison of autoadhesion (peel strength) and surface composition (from XPS data) for LDPE discharge treated in air, nitrogen and argon. Heat seals were made at 75°C and 15 psi with 2 s contact time. The $\text{O}_{1s}:\text{C}_{1s}$ intensity ratio is a qualitative measure of surface oxidation level. $\text{N}_{1s}:\text{C}_{1s}$ ratios refer only to surfaces treated in nitrogen. Note that similar surface oxidation level for samples giving peel strengths of $100 \text{ gm}/25 \text{ mm}$ (---), (broken lines)

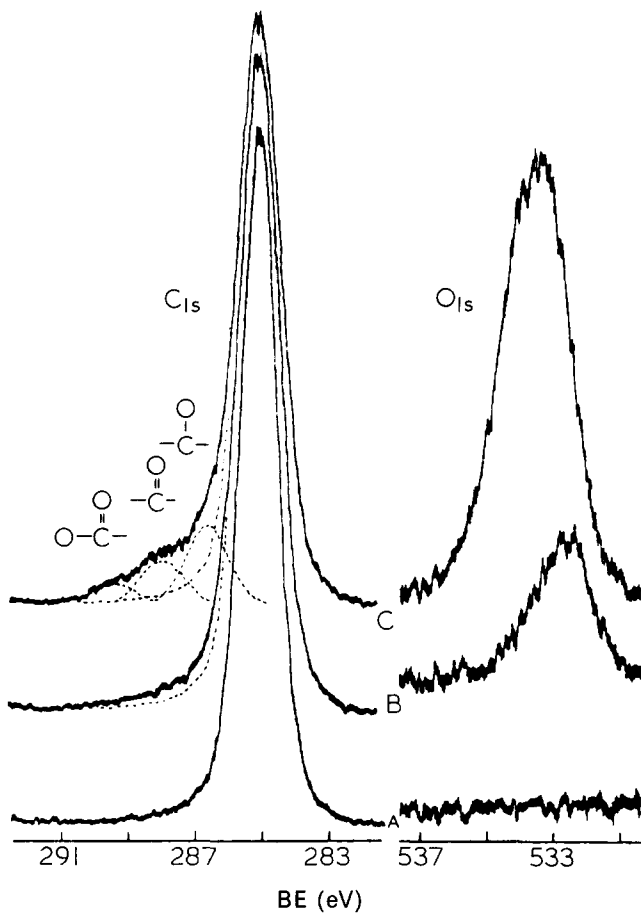


Figure 3 High resolution C_{1s} and O_{1s} spectra for LDPE (A) untreated (B) and (C) discharge treated in air (13.7 kV peak voltage 50 Hz) for 8s and 30s respectively. Count rates are 3×10^3 counts s^{-1} FSD (C_{1s}) and 10^3 counts s^{-1} (O_{1s}). Lack of specificity in the high binding energy C_{1s} peaks is indicated by the following: >C-O could be alcohol, enol, ether, alkyl ester, peroxide, hydro peroxide, etc. >C=O could be ketone or aldehyde, -CO-O could be carboxylic acid or ester, or peracid

tration. Although different treatment times are involved, the power dissipated for a particular value of peel strength is independent of the gas used. XPS also showed that treatment in a hydrogen atmosphere did not lead to introduction of oxygen and no auto-adhesion enhancement resulted¹⁵. This work clearly gave the Owen's theory a firmer foundation but a more complete analysis of oxygen functionalities was required to confirm the details. High resolution C_{1s} and O_{1s} spectra from typical air-treated surfaces are shown in Figure 3. Two points emerge from these spectra. Firstly, easily observable structure from oxygen functions in the C_{1s} spectrum is only obtained after treatment levels significantly in excess of those at which autoadhesion is developed (compare Figures 2 and 3). Secondly, even when spectral changes are pronounced the O_{1s} peak is uninformative because most oxygen functional groups give O_{1s} BE's around 532 eV, the major exception being -C(=O)-O at ~ 533.5 eV;

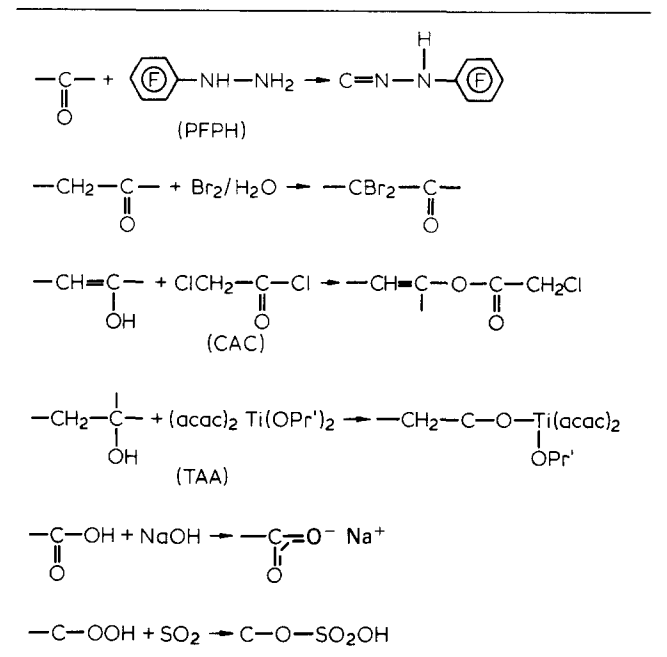
moreover the deconvoluted C_{1s} spectrum is ambiguous as noted in Figure 3.

The derivatization reactions developed to probe the functionality of these surfaces are listed in Table 1. Full

experimental details can be found in refs. 10 and 11. The consensus view in the literature for the likely mechanism during discharge treatment of LDPE is shown in Figure 4. Both chain scission and crosslinking take place. The key intermediate is the hydroperoxide group, whose stability and decomposition has been the subject of much research. Hydroperoxides in polyethylene can have long lifetimes, so if this mechanism is correct these groups should be detectable. The SO_2 reaction is positive identification and, we believe, the first direct evidence for this mechanism. Of the groups likely to be produced by hydroperoxide decomposition, derivatization techniques have therefore identified >C=O , -C-OH and -COOH and have also shown that -C=C-OH can be formed (by keto-enol tautomerization).

The XPS data can be quantified, as previously described¹¹, to give the data in Table 2. The value for the population of $\text{CH}_2\text{C=O}$ groups assumes that on average two α -H atoms will be replaced during bromination. Since this group can tautomerize to give one enol -OH the population of $\text{-CH}_2\text{C=O}$ assessed by Br_2 uptake and enolic -OH assessed by the CAC reaction should be comparable, as is observed. The raw C_{1s} spectra tend to show broadly similar intensities for the C-OH (etc),

Table 1 Derivatization reactions employed



Abbreviations: PFPH = pentafluorophenylhydrazine
CAC = chloroacetylchloride
TAA = di-isopropoxytitanium bisacetylacetonate

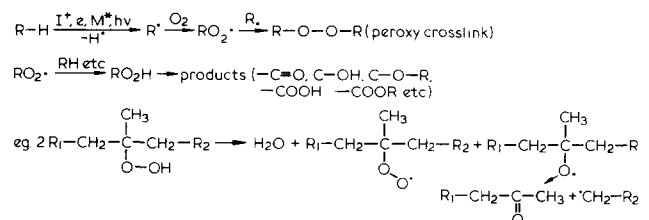


Figure 4 Likely mechanism of discharge treatment

Table 2 Quantification of functional groups

Reaction	XPS ratio [†] (core level/C1s)	Atomic ratio (element/carbon)	Number of functional group per original surface —CH2—
PFPH	(F _{1s}) 0.205	5.5 × 10 ⁻²	>C=O, 1.1 × 10 ⁻²
Br ₂ /H ₂ O	(Br _{3d}) 3.6 × 10 ⁻²	10.6 × 10 ⁻³	CH ₂ C=O, 5.3 × 10 ⁻³
CAC	(Cl _{2p}) 1.3 × 10 ⁻²	6.0 × 10 ⁻³	C—OH, 6.0 × 10 ⁻³
TAA	(Ti _{2p3/2}) 6.2 × 10 ⁻²	1.5 × 10 ⁻²	C—OH, 1.5 × 10 ⁻²
NaOH	(N _{1s}) 8.8 × 10 ⁻²	1.1 × 10 ⁻²	—COOH, 1.1 × 10 ⁻²
SO ₂	(S _{2p}) 7.6 × 10 ⁻³	4.7 × 10 ⁻³	C—OOH, 4.7 × 10 ⁻³
None	(O _{1s}) 0.209	8.7 × 10 ⁻²	

[†] Estimate error ± 5% for a given sample, ± 15% for the complete experiment

Table 3 XPS and auto-adhesion measurements from derivatized surfaces

Treatment	C _{1s} (3 × 10 ⁴)	O _{1s} (10 ⁴)	F _{1s} (10 ⁴)	Ti _{2p3/2} (3 × 10 ³)	Peel strength [†] (g/25 mm)
DT	20.4	12.8	—	—	250
DT-PFPH	20.0	7.5	12.3	—	0
DT-PFPH-TAA	18.7	11.2	9.7	15.2	241
DT-TAA	19.8	12.9	—	15.3	390
DT-TAA-PFPH	18.8	15.0	9.1	11.6	180

[†] Estimate error ±5%, for discharge treated samples, ±10–15% for derivatized samples

C=O and —COOH regions which is also borne out by these results. The total assay of C=O, C—OH and COOH groups would give an atomic O:C ratio of 5.7 × 10⁻² where 'C' is the carbon atoms in the original surface. This compares with the actual value of 8.7 × 10⁻² from the discharge treated surface. Considering that ether and ester groups are also likely to be present, in numbers comparable with the groups which have been derivatized, this assay is seen to be entirely reasonable. The apparent internal consistency of these results is additional evidence for the essential reliability of the derivatization procedures used.

The derivatization technique as developed for the extension of XPS analytical capacity has the added bonus that the same surfaces can be used to study specific interactions in adhesion, in the spirit of Owens' approach¹⁴, but with a built in monitor of surface composition. This overcomes the possibility that artefacts, such as contamination, loss of surface material, or solvent-induced re-orientation effects could be responsible for the observed adhesion changes—artefacts that Owens' experiments could not rule out.

We first used these techniques to show¹⁰ that hydrogen bonding between carbonyl and enol functions on opposite discharge treated LDPE surfaces was responsible for auto-adhesion, as postulated by Owens¹⁴. The results also showed that the required keto-enol tautomerization occurred. In this work we also showed⁹ that the blocking of enol functions prevented adhesion between discharge treated LDPE and a commercially obtainable printing ink. We then extended this investigation of the role of specific interactions using the auto-adhesion between discharge treated LDPE surfaces as a model system¹¹.

It should be emphasised that under the conditions of heat sealing used (at 85°C) untreated LDPE surfaces do

not auto-adhere, in other words an interdiffusion mechanism is unlikely.

Table 3 shows the effect on adhesion of reacting the surfaces with PFPH and TAA. As reported earlier PFPH prevents adhesion by eliminating enolizable carbonyl groups. Alternatively, reaction with TAA actually increases adhesion above that of the discharge treatment alone. This would be consistent with the opening of another specific interaction 'channel', namely crosslinking of —OH groups via the Ti complex. Since the above analysis suggests that enolic and alcoholic —OH groups can be separately derivatized, then reaction with PFPH and TAA should give independent control over these two sites for specific interaction. This is clearly seen in the case of sequential reaction with the two reagents. Despite the increased error involved in carrying out two solvent based derivatization reactions the XPS data are reasonably self-consistent also.

The point of this minor digression is to emphasize the role of XPS with derivatization in adhesion studies, probably the major area of polymer surface and interface research.

STATIC SIMS OF POLYMER SURFACES

As noted above SIMS has several potential advantages over XPS for polymer surface analysis, namely: greater molecular specificity (via fingerprint spectra), greater surface sensitivity (1–2 monolayers) and the capacity to operate at high spatial resolution. However, there are several practical problems which stand in the way of realizing this potential, namely: the expected high rate of ion beam damage and the need for charge neutralization—which in turn leads to uncertainty of surface potential and the possibility of electron stimulated ion emission (ESIE). Early work by Gardella and Hercules^{17,18} did indeed suggest that the first two of the

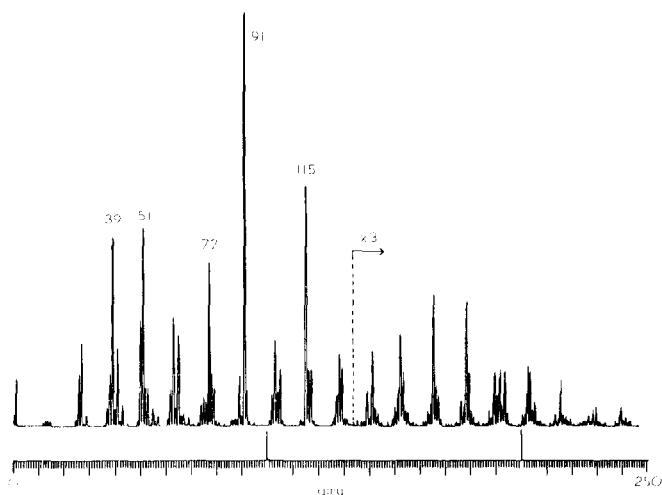


Figure 5 Positive secondary ion mass spectrum of polystyrene (see text for conditions) (3×10^3 counts s^{-1} f.s.d.)

above advantages could be realized, although their optimistic conclusions were probably not completely justified (see below). The problems described above have been systematically studied in the author's laboratory in order to determine their magnitude and the scope for their solution. It is sufficient at this time to summarize the experimental conditions, determined as a result of this study¹⁹, which allow reproducible SIMS examination of polymer surfaces. It should be noted that these conditions are appropriate to analyses where spatial resolution is not an issue. Imaging is specifically addressed in a later section.

The apparatus used for this work is based on the VG Scientific ESCALAB Mk 1, capable of carrying out MgK α and AlK α excited XPS, and fitted with an AG 61 differentially pumped, non-mass filtered, ion gun (giving a focussable beam of $\sim 30 \mu\text{m}$ minimum diameter) and an MM 12-12 quadrupole mass spectrometer with a range of 1–800 amu for SIMS. Charge neutralisation is effected with a LEG31 electron gun. The conditions arrived at as being optimal for polymer analysis are as follows: A 4 keV Ar⁺ beam is defocussed and rastered to give the maximum area of irradiation (≈ 5 mm square, or $\sim 0.3 \text{ cm}^{-2}$). The ion current is typically 0.3–0.6 nA. The electron beam, accelerated to 700 eV, is operated at the minimum preset current rating of $1 \mu\text{m}$, and defocussed so that a static beam floods an area of the sample much larger than the region irradiated by the ion beam (typically 1 cm^{-2}). The exact current density is varied by adjustment of the filament current, but is typically $< 5 \text{ nA cm}^{-2}$ and around three times the ion beam current density. Under these conditions spectra with the quality of Figure 5 are routinely obtainable, base peaks having intensities typically between 10^3 and 3×10^4 counts s^{-1} depending on the material. High mass clusters having intensities of < 100 counts s^{-1} can still be observed readily because the background count rate is so low.*

The spectrum of polystyrene (PS) shown in Figure 5 was obtained in 300 s. Usually both positive and negative ion spectra are recorded in less than 500 s, corresponding to an ion dose of $\sim 2 \times 10^{12}$ ions cm^{-2} under the highest current conditions used. This is well inside the domain dubbed as 'static SIMS' by those working in the adsorption field, but obviously the damage to organic

surfaces is rather different since the radicals formed by charged particle impact are reactive species which can lead to structural changes in the polymer by further reaction. Experiments in which XPS was used to follow ion-beam damage to PS under SIMS conditions¹⁹ suggest a lower limit to the ion dose required to cause changes to the secondary ion spectrum of $\sim 10^{13}$ ions cm^{-2} . A systematic study of ion beam damage rates for a variety of polymer types is now underway.

Within the time scale required for SIMS analysis the conditions described above provide a stable surface potential. However, the sample surface potential can be altered by the sample bias which is usually required to optimise spectral intensities (by matching secondary ion energy distribution maxima to the acceptance energy of the quadrupole mass filter). This change in surface potential affects relative peak intensities¹⁹, particularly of low mass clusters, as shown in Figure 6 and this can be important when intensities of peaks are used for structural analysis, e.g. the differentiation of isomeric species. Under the experimental conditions described it is rare for ESIE to make a significant contribution to the secondary ion mass spectrum, and, in any case, ESIE is generally confined to low mass species (PTFE is a notable exception)²⁰.

Fingerprint spectra

The positive ion mass spectra from some pure polymer film surfaces, obtained under the conditions described above are shown in Figures 7–13. Taken together with Figure 5 (PS) and Figure 6 (essentially the spectrum of low density polyethylene, LDPE), a wide range of chemical types are covered. It is not appropriate here to go into detailed interpretations of these spectra (this has been done elsewhere^{19–22}), but some prominent and characteristic peaks can be identified which will be useful in subsequent discussion.

Starting with poly(methacrylic acid) (PMAA), shown in Figure 7, the peak at 101 amu corresponds to $[\text{C}_4\text{H}_8\text{COOH}]^+$, a structural unit, with 57 amu, C_4H_9^+ , arising from the expulsion of CO_2 . The C_3 triplet of 39, 41, 43 amu (C_3H_3^+ , C_3H_5^+ , C_3H_7^+) is common to polymers with hydrocarbon backbones (cf. Figure 6) and such polymers with β -methyl-substituted backbones have a prominent peak at 69 amu, as seen for PMAA.

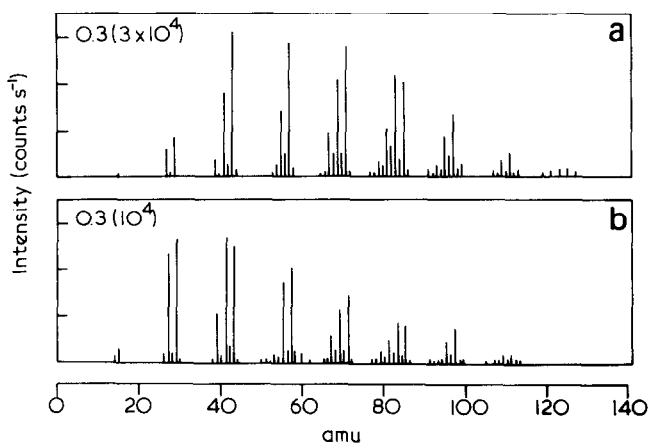


Figure 6 Positive secondary ion mass spectra from thin (conducting) paraffin wax film. Target bias of 12.5 V (a) and 7.5 V (b)

* See note added in proof

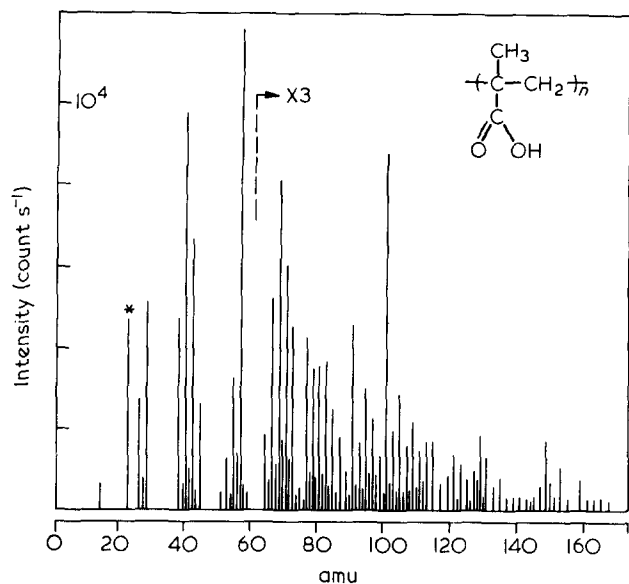


Figure 7 Positive SIMS of poly(methacrylic acid). * Na⁺

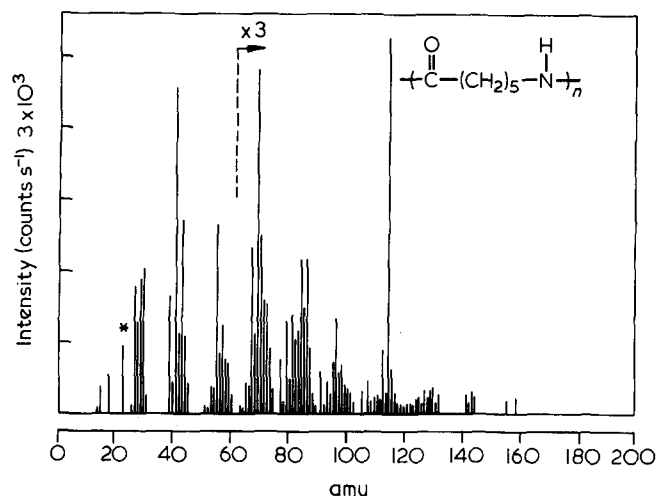
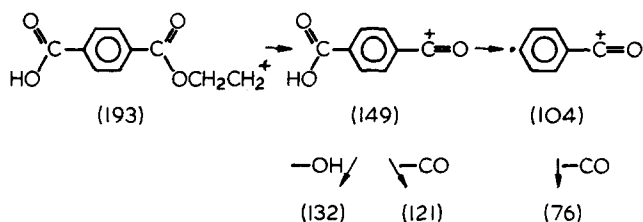


Figure 8 Positive SIMS of nylon-6. *Na⁺

For nylon-6, 114 amu corresponds to MH⁺ where M is the monomer unit, ε-caprolactam. Peaks at 55 amu (C₂H₃CO⁺) and 30 amu (H₂NCH₂⁺) reflect the presence of the peptide unit (Figure 8). The poly(ethylene terephthalate) (PET) spectrum, Figure 9, is elegantly simple. Peaks at 193 and 191 amu correspond to (M+H)⁺ and (M-H)⁺ with fragmentation following paths such as:



The other aromatic system, PS (Figure 5) has characteristic peaks at 91 amu due to C₇H₇⁺ (cyclic tropylium ion) and 115 amu due to C₉H₇⁺ with the structure:

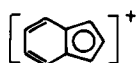
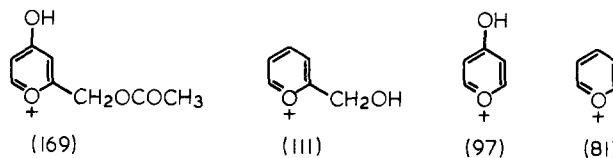


Figure 10 shows the spectrum of cellulose triacetate, a film forming polymer made by the acetylation of the natural polysaccharide cellulose. Spectral domination by 43 amu (CH₃CO⁺) and 15 amu (CH₃⁺) indicates the importance of side chain fragmentation. A series of prominent peaks can be assigned:



which points to the stabilization effect of the aromatic heterocyclic ion which can be derived from the saccharide unit. It should perhaps be noted that the idealized repeat unit for cellulose triacetate is:

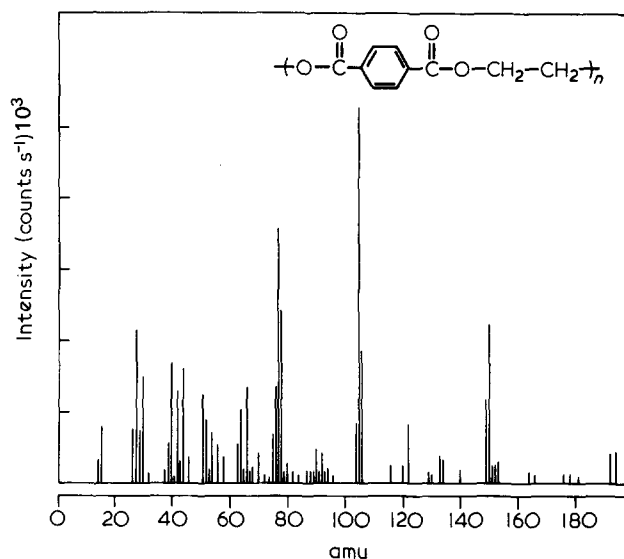
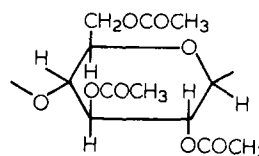


Figure 9 Positive SIMS of poly(ethylene terephthalate)

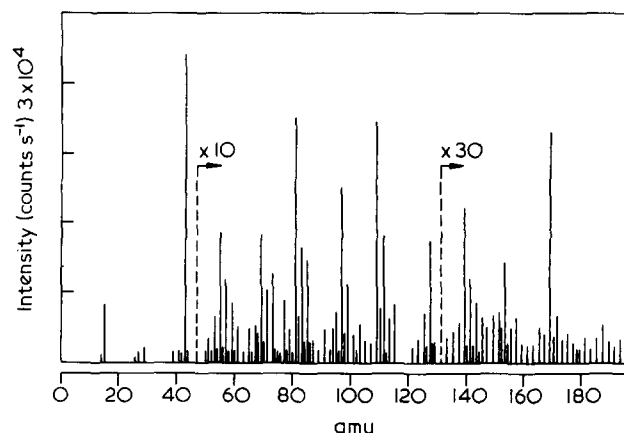


Figure 10 Positive SIMS of cellulose triacetate

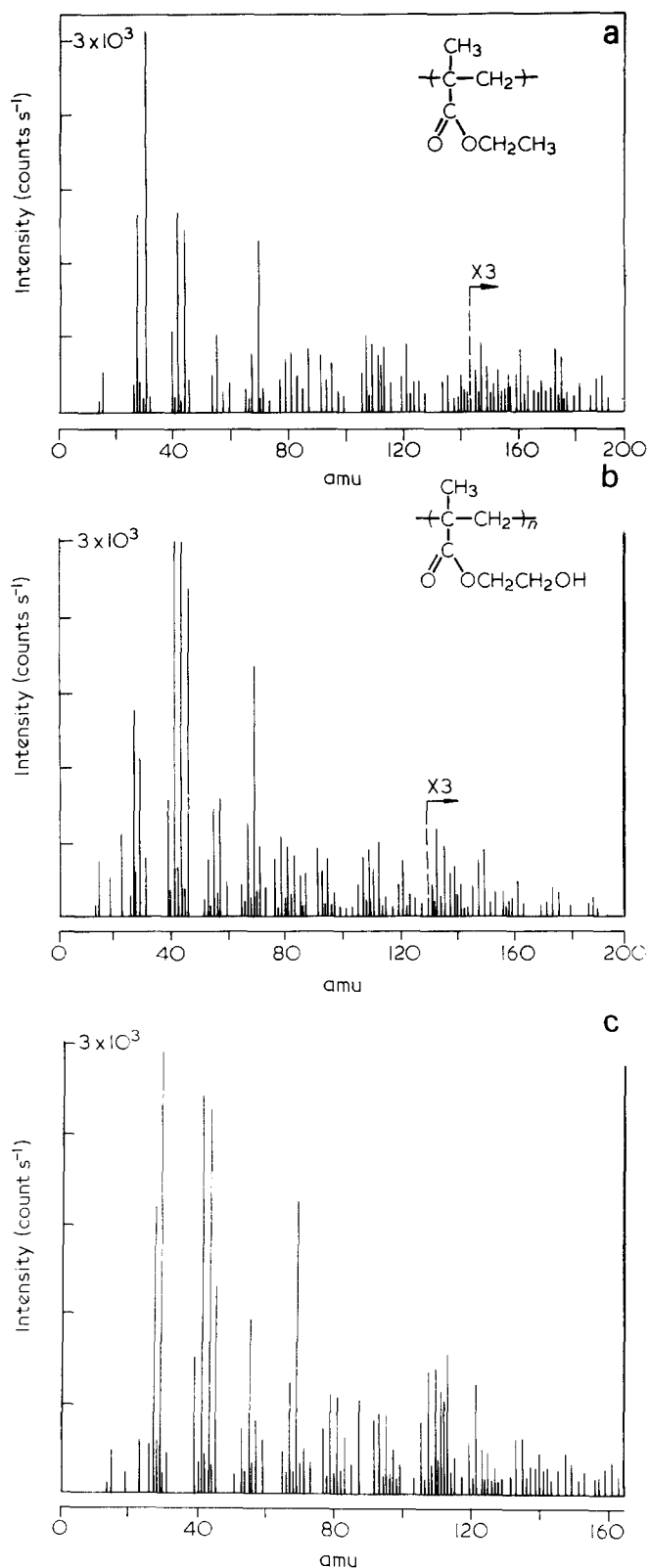


Figure 11 Positive SIMS of (a) poly(ethylmethacrylate), (b) poly(hydroxyethylmethacrylate), (c) a 1:1 copolymer of ethyl- and hydroxyethylmethacrylate

but the commercial 'triacetate' has slightly less than 3 acetyl groups per unit and indeed the detailed structure of the polymer is still uncertain. In this context however these details are of no importance.

The three spectra in Figure 11: poly(ethylmethacrylate) (PEMA), poly(hydroxyethylmethacrylate) (PHEMA) and a 1:1 random copolymer of these two monomers again

show the importance of side chain fragmentation with the prominence of 29 amu (C₂H₅⁺) for PEMA, 45 amu (C₂H₄OH⁺) for PHEMA. The copolymer spectrum is essentially equivalent to the addition of these two spectra.

Figure 12 shows the spectra from two commercial samples of silicone oil. One is a pure poly(dimethylsiloxane) (ICI F111/1000) with prominent peaks at 73

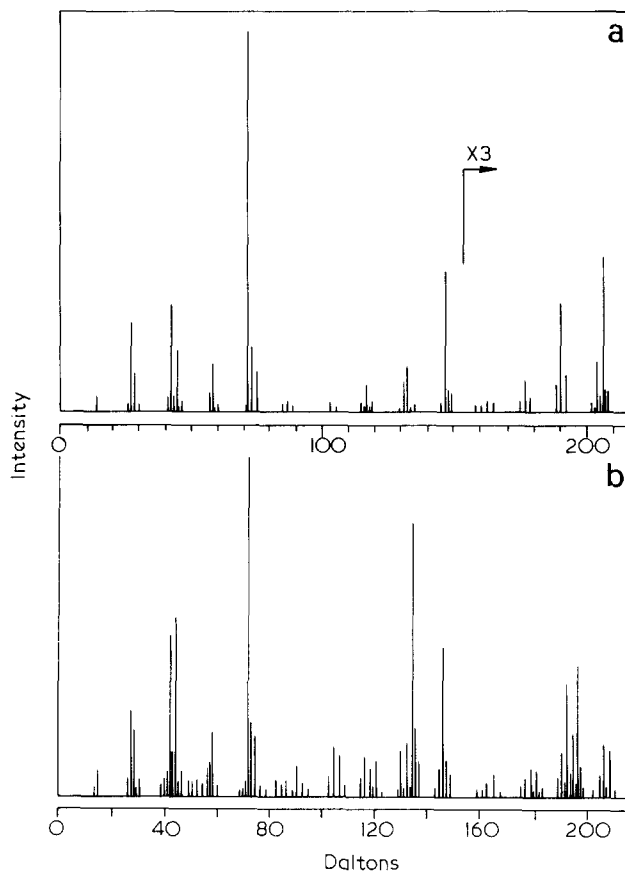


Figure 12 Positive SIMS of (a) dimethylsilicone (b) phenylmethylsilicone (see text) (10³ counts s⁻¹ f.s.d.)

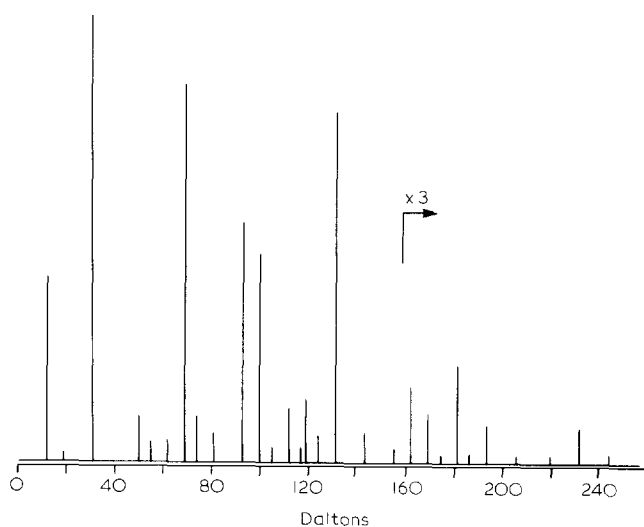


Figure 13 Positive SIMS of poly(tetrafluoroethylene) (10⁴ counts s⁻¹ f.s.d.)

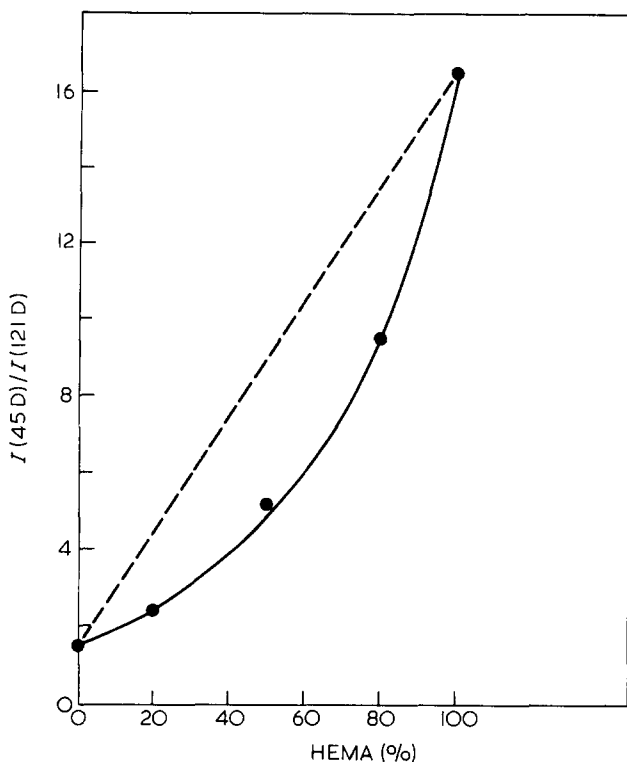


Figure 14 Variation of 45D/121D peak intensity ratio (positive ions) with composition of EMA:HEMA random copolymers

amu and 147 amu due to: $(\text{CH}_3)_3\text{Si}^+$ (73) and $(\text{CH}_3)_3\text{Si-O-Si}(\text{CH}_3)_2^+$ (147).

The other, Dow Corning 710, is described by the manufacturers as a phenylmethylpolysiloxane (purity unknown). It has, in particular, the additional unique peak at 135 amu due to: $(\text{CH}_3)_2\text{PhSi}^+$.

Finally, the spectrum of polytetrafluoroethylene (PTFE) is shown in Figure 13. Unusually this has a distinct peak at 12 amu (C^+) with the other peaks following C_nF_m^+ (CF^+ , CF_2^+ , C_2F_3^+ , C_3F_4^+ , C_3F_5^+ at 31, 69, 93, 100, 131 amu respectively).

It can be stated in summary, that prominent peaks in positive secondary ion mass spectra of polymers are closely related to simple structural units (i.e. the original monomer) and that fragmentation patterns are usually easily recognized by reference by electron impact (EI) mass spectral data from related molecules. A recently completed study of polymethacrylates has probed in detail the relative contributions of the polymer backbone and the ester side chain to the positive ion mass spectrum and has resulted in some understanding of cluster ion formation mechanism²³. These materials featured in the early work of Gardella and Hercules on SIMS analysis of polymers^{17,18} and it now seems clear that the information content of their spectra was significantly reduced through the accumulation of excessive ion doses²³.

Although negative ion spectra are usually restricted to a few low mass peaks, they are useful. Halogens are readily detected, of course, and the relative intensity of O^- and OH^- peaks are a reasonable guide to oxygen content. A strong peak at 26 amu (CN^-) is usually indicative of nitrogen content. It can also be mentioned that in cases where analysis at high spatial resolution is not required fast atom bombardment mass spectrometry (FABMS) is a preferable technique because it avoids the complications of electron beam charge neutralization. Equivalent

spectra to SIMS are obtained, and samples in powder form (often difficult to charge neutralise for SIMS analysis) can be easily studied²⁴.

A criticism frequently levelled at SIMS as an analytical technique is the difficulty of quantification, resulting from pronounced matrix effects on ion yields. It is too early in the development of the technique in this field of materials science to comment on the likelihood that these problems will be overcome. However, results from a close re-examination²³ of the complete range of random copolymers containing EMA and HEMA (see Figure 11), taking extreme care to impose identical experimental conditions during spectral acquisition, give reason for optimism. Taking the intensity ratio of the peaks at 45 amu ($\text{C}_2\text{H}_5\text{OH}^+$, essentially specific to HEMA) and 121 amu (structure uncertain, but essentially due to the common methacrylate backbone) gives the correlation with structure shown in Figure 14. The departure from linearity may be a matrix effect or may actually represent a real difference in surface and bulk compositions.

Applications

Despite the very recent development of these techniques, they are already finding routine application in the author's laboratory. A fruitful area concerns polyester film surface analysis. Biaxially oriented poly(ethylene-terephthalate) (PET) film (e.g. ICI Melinex®, Du Pont Mylar®) is used in a very wide range of products such as packaging films, photographic films, reprographic materials, audio and video magnetic tapes, electrical components and credit cards to name only a few. Many of these uses require surface properties not processed by the original polyester, e.g. heat sealability at low temperature, high levels of adhesion, low surface resistivity. These properties are achieved by surface treatment, in a variety of ways, or by depositing 'effect' molecules onto the surface. Frequently these surface modifications are <100 Å in thickness, with a tendency to discontinuity. Clearly, also, surface contamination can have a very serious effect on these material properties.

Figure 15 shows XP-spectra for the two surfaces of a PET film modified on one surface for adhesion enhancement. The modified region is too thin for analysis by reflection-i.r. spectroscopy (sampling depth >1 μm) but thick enough to obscure the substrate when examined by XPS. Even so, differences in the C_{1s} and O_{1s} spectra from the two sides are marginal, and only readily observed at the highest spectral resolution. Little information about the structure of the modified surface can be obtained from the XP spectra. The SIMS spectrum of the modified surface is shown in Figure 16 whilst the quite unique PET spectrum has been discussed from Figure 9. These unique spectral fingerprints also allow patchy (discontinuous) overlayers to be studied whereas XPS is a non-starter unless the overlayer contains components which give rise to distinctive core-level peaks (i.e. other than C_{1s} and O_{1s}).

Another example of this, which also covers contamination effects is illustrated by Figure 17. PET film modified on one surface for adhesion enhancement to low density polyethylene was used by a film converter to make PET-LDPE laminate. Poor adhesion results raised the possibility that lamination to the unmodified PET surface had been done by mistake. XPS data were surprisingly ambiguous, when used to determine the composition of the non-LDPE surface of the laminate. Spectra uncharac-

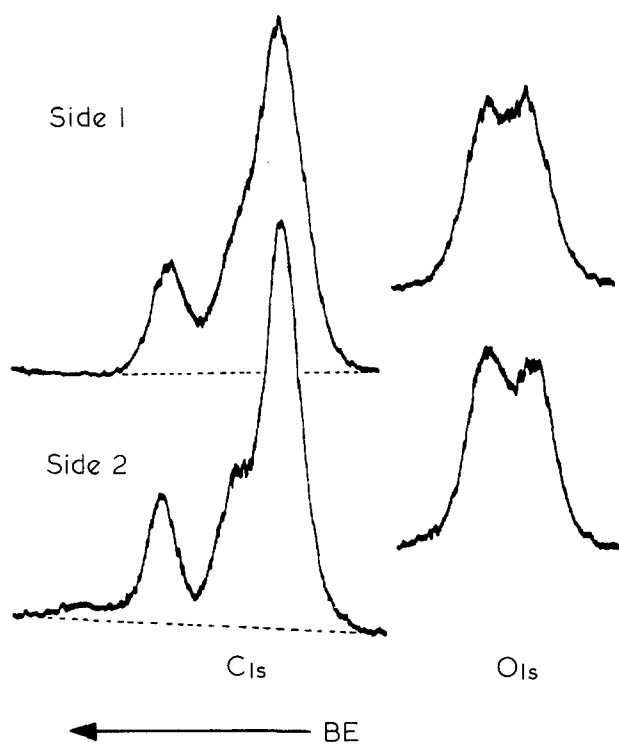


Figure 15 High resolution C_{1s} and O_{1s} spectra from the two surfaces of PET film chemically modified on side 1

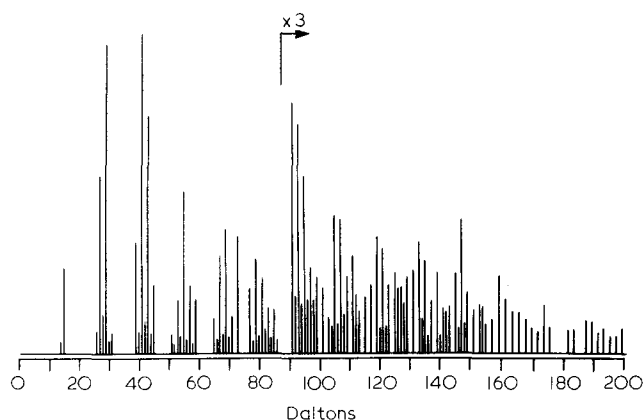


Figure 16 Positive SIMS of PET film side 1 of Figure 15

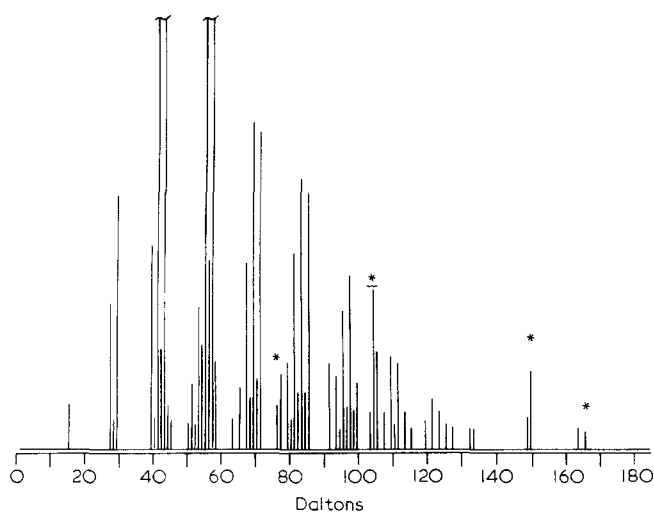


Figure 17 Positive SIMS of PET surface contaminated with LDPE (10^3 counts s^{-1} f.s.d.) * Denotes peaks characteristic of PET (cf. Figure 9)

teristic of both PET and the modified surface (also containing only C/H/O) were obtained. The SIMS results explained why. Figure 17 shows that the surface is PET contaminated with hydrocarbon, resulting from transfer of low molecular weight material from the LDPE layer to the PET surface during contact in the reeled laminate (cf. Figures 6 and 9). Surface contamination by material transfer between asymmetrical film surfaces in reels is a common problem.

A third problem concerns the identification of deposited 'effect' molecules. Figure 18 shows the wide scan XP-spectrum of a polyester surface displaying low surface resistivity. The only peaks additional to the polyester C_{1s} and O_{1s} are small N_{1s} and Cl_{2p} peaks, the inset shows the complex N_{1s} signal. In total the N and Cl surface concentrations are only approximately 4 and 0.5 atomic percent respectively (H not included in assay). The N_{1s} BE's are not unambiguous, but on the basis of experience the three peaks can be most likely assigned to NO_3^- (~ 406 eV), R_3N^+ (~ 402 eV) and $-NH_2$, $-CONH-$ or $-CN$ (~ 399.5 eV). The Cl_{2p} at ~ 198 eV certainly represents Cl^- . $LiNO_3$ is a possible component of an antistatic formulation but Li at the appropriate level is undetectable by XPS. Moreover the N_{1s} peak assigned to NO_3^- was very sensitive to X-ray exposure making quantification difficult. The positive secondary ion mass spectrum is shown in Figure 19. Immediately the absence of Li^+ (7 amu) is obvious, but characteristic peaks from PET are also absent. This illustrates the markedly enhanced surface sensitivity of SIMS relative to XPS. Using the XPS data possible candidates for the antistatic agent were identified and the SIMS spectrum of one, analysed after spreading onto a substrate, matched that in Figure 19. Given an adequate data base, such as exists in

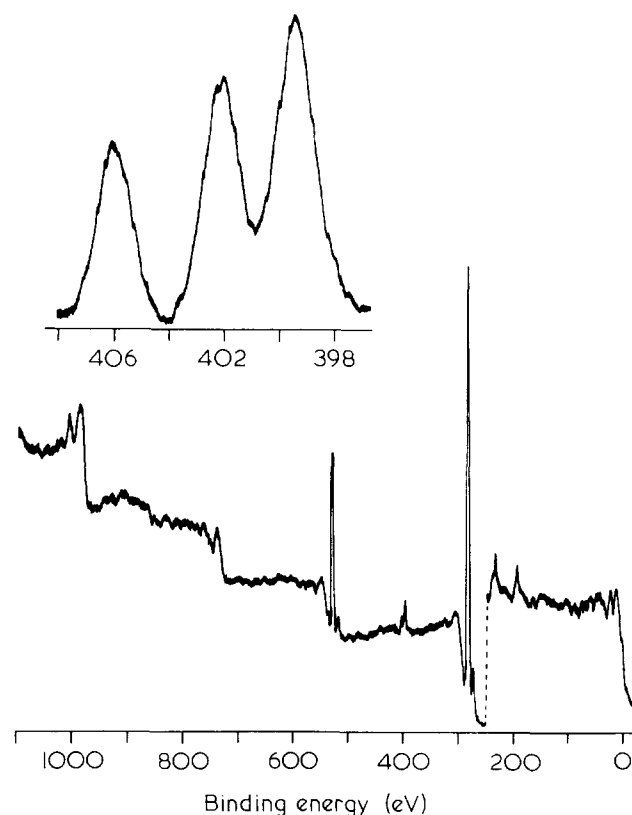


Figure 18 XPS survey scan of antistatic PET film surface: inset expands the N_{1s} region

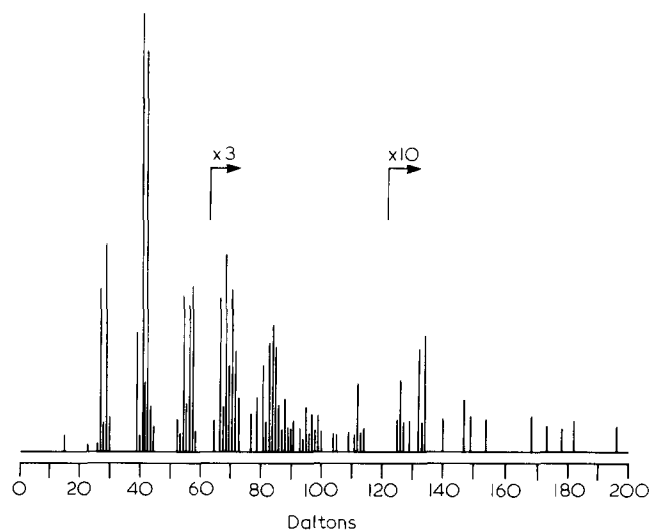


Figure 19 Positive SIMS of antistatic PET film surface (cf. Figure 18)

conventional mass spectrometry or infra-red spectroscopy, it is clear that SIMS fingerprinting represents an extremely sensitive tool for the identification of complex molecules on surfaces.

A further example of contamination detection is the following. In order to discuss the interactions of polyethersulphone (PES) with fibre surfaces in composite materials it is necessary to characterize the surface energy of the polymer. The advantages and disadvantages of various contact angle based measurement techniques for doing this have been discussed by Bystry and Penn recently²⁵, but for a polymer melting in the region of 300°C and difficult to cast from solution the best methods described are inappropriate. We have attempted the characterization of oriented PES film surfaces which have the required smoothness. Figure 20(a) shows part of the XPS-spectrum of film freshly cut from a reel and thoroughly water washed. High resolution C_{1s}, S_{2p}, and O_{1s} spectra were as expected for the repeat unit and no contaminant peaks were observed. Figure 20(b) however, shows the positive secondary ion spectrum which clearly shows the presence of dimethylsilicone contamination (see Figure 12(a)). Attempts at further cleaning of the PES surface which resulted in a decrease in intensity of the silicone signals did markedly change contact angle (especially hysteresis) results, emphasising the importance of low contamination levels on these measurements.

TECHNIQUE COMBINATION AND OTHER XPS DEVELOPMENTS

Several of the above examples indicate the advantages of having both XPS and SIMS available for sequential study of polymer surfaces. This has been particularly important during the development of SIMS, but the advantages will remain. The great virtues of XPS are in the ease of element detection and quantification, the complementary virtues of SIMS are fingerprint specificity and sensitivity.

The lack of spatial resolution in XPS is now being attacked and recent work has demonstrated 'small area analysis' from regions of ~250 μm in dimension (although not from polymers)²⁶.

A major problem in the field is the study of vertical inhomogeneity by depth profiling. Use of inert gas etching

is generally inappropriate because polymers degrade rapidly to carbon which then has a very low sputtering rate. Non-destructive depth profiling by angular variation experiments in XPS is very important where appropriate and this can be enhanced by the use of high energy X-ray excitation which leads to a greater maximum sampling depth. Clark has reported on the use of TiKα (4.5 keV) for this purpose². Spectral interpretation is made more complicated by the width and doublet nature of the exciting X-ray line but the recent development²⁷ of a monochromated AgLα source means that this problem can be solved, albeit for a photon with somewhat lower energy (3 keV). Advances are also being made in the quantitative interpretation of angular variation data from polymeric systems^{28,29} which will significantly aid the exploitation of these developments.

SECONDARY ION IMAGING AND MICRO-ANALYSIS

The technique for SIMS analysis of polymer surfaces discussed so far involves rastering a focussed beam within a region flooded with neutralizing electrons. Imaging should be a relatively simple matter of tuning the mass

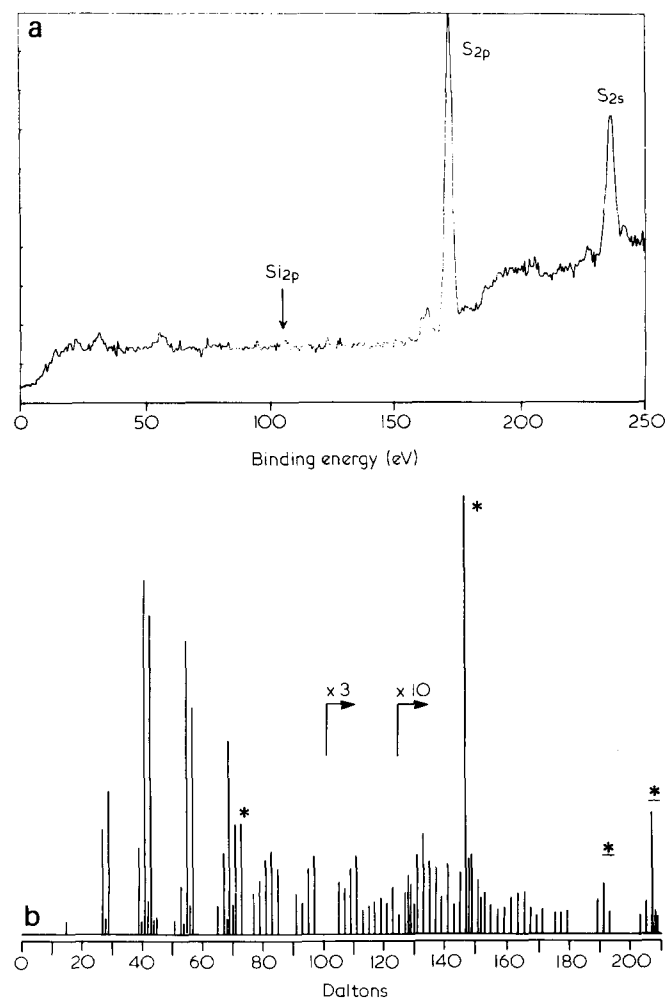


Figure 20 (a) XPS of water washed poly(ethersulphone) (PES) film surface in the 0–250 eV region. Scale expansion shows a Si_{2p} signal to be just detectable (Si_{2p}/S_{2p} intensity ratio=0.02). An Si concentration of ~0.2 atomic % (H excluded) is calculated to be present. (b) Positive SIMS of PES surface. * Denotes peaks characteristic of dimethylsilicone (cf. Figure 12)

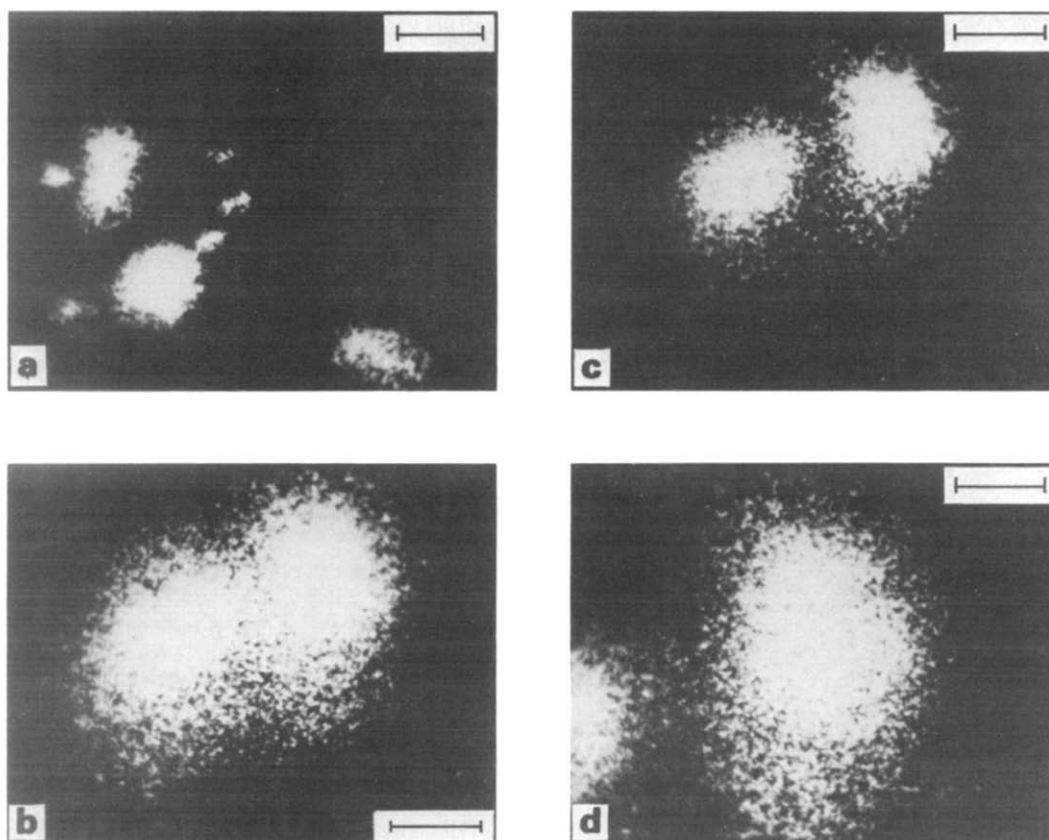
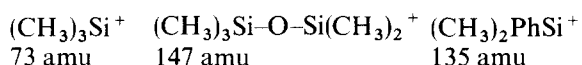


Figure 21 Images of Dow Corning 710 silicone oil spots on LDPE using 4 KeV Ar⁺ (50 pA) and 700 eV electron flood (variable flux but 6 nAcm⁻² maximum). Each image is the accumulation of 2 × 100s scans; (a) positive ions of 73d, bar=1 mm; (b) as (a), bar=100 μm, double spot is at centre of (a); (c) as (b), bar=100 μm, but using positive ions of 135d; (d) as (c), bar=50 μm, right hand spot of (c) imaged

spectrometer to a chosen m/z value and using the ion current to modulate an oscilloscope display. In fact, this has been achieved recently²¹ with a spatial resolution essentially limited by the spot size of the ion beam, as illustrated below.

Silicone contamination of polymer surfaces is a frequent problem, particularly when present in the form of isolated small drops from aerosol deposition. This leads to highly localized adhesion failure for coatings, ink etc. and to optical defects. Silicones are also stress-cracking agents for low density polyethylene. Microanalysis of these materials is therefore a realistic objective.

Two different viscous oils were used in these experiments; one a pure dimethylsilicone (poly(dimethylsiloxane)) (ICI F111/1000) the other, Dow Corning 710, described by the manufacturers as a phenylmethylpolysiloxane (purity unknown). Spectra of the neat oils spread very thinly on LDPE are shown in *Figure 12*; that of the dimethylsilicone is essentially identical to the electron impact (EI) mass spectrum of volatile components which has been fully assigned³⁰. For the purposes of these experiments high intensity signals of fingerprinting significance are:



The 135 amu peak is clearly unique to the Dow Corning 710 silicone. It should be noted that ESIE was negligible for these materials. *Figure 21* shows images from an LDPE sample spotted, using a fine wire, with the Dow

Corning 710 oil. The apparent increase in spatial resolution when using the 135 amu peak may be a sputtering artifact. Nevertheless a spatial resolution of ~50 μm is indicated.

Figure 22 shows images from a similar sample with three slightly larger oil spots using both types of silicone²¹. In these images the dot brightness of the storage oscilloscope has been made over-intense to minimize image collection time: at the cost of image quality. The 73 amu peak images both silicones whilst the 135 amu peak is specific to the Dow Corning 710 silicone. This is sufficient to identify which spot corresponds to which silicone, but *Figure 23* shows complete spectra from localized areas. *Figure 23(a)* was obtained by holding the sample at the position corresponding to *Figure 22(a)* but increasing the magnification by ×2.5 and rastering at TV rate, effectively sampling only the large spot. *Figure 23(b)* was obtained by rastering at TV rate over the area imaged in *Figure 22(c)* thus sampling mainly one of the small spots, but with some LDPE contribution. These spectra can be compared with those in *Figure 12* and the spectrum of LDPE reported previously²⁰ and essentially reproduced in *Figure 6*.

Mapping of organic species clearly only requires that one unique peak for each component can be selected from the mass spectra. The use of a high mass-range quadrupole mass spectrometer allowing good transmission of high mass species is therefore essential to increase the probability that such unique species can be observed. There are still practical difficulties to overcome, particularly with respect to charge neutralization, but the

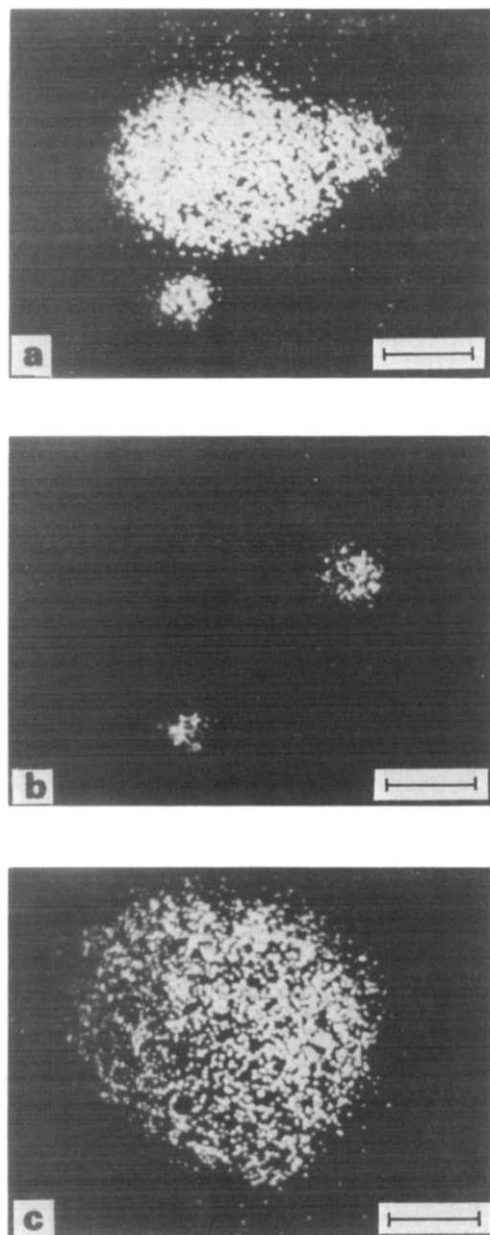


Figure 22 Images of mixed spots of silicone oils on LDPE (see text) using positive ions at 73d (a) and 135d (b) and (c). In all cases 4 keV Ar^+ and 700 eV electron flood. Conditions: (a) ion current (I_i) = 0.1 nA; electron current (I_e) = 1 nAcm^{-2} , 2×100 s scans, bar = 500 μm . (b) I_i = 0.1 nA, I_e = 1 nAcm^{-2} , 3×100 s scans, bar = 500 μm . (c) I_i = 50 pA, I_e = 3 nAcm^{-2} , 1×100 s scan, bar 100 μm , (a) and (b) are equivalent images, (c) magnifies the upper spot in (b)

potential of this technology for problem solving around polymeric/organic materials is immense.

Recently, the advent of liquid-metal ion sources has reduced significantly the dimensions of primary ion beams for this type of work. *Figure 24(a)* shows the Ga-ion induced SEM from a carbon fibre/thermoplastic polymer fracture surface³¹. The ion beam spot size used here was $\sim 0.5 \mu\text{m}$. Many fibres have been pulled out apparently cleanly from the matrix but some have a rough surface indicating adhered polymer. *Figures 24(b)* and (c) show secondary ion images of the same area using negative ions characteristic of the fibre surface (C_2H_2^- from graphite) and of both the fibre and the polymer (C_2^-). There are obvious shadowing effects but it is clear that

regions in the SEM which appear to show fibre covered by polymer, show up as dark regions in the C_2H_2^- image. The C_2^- ion which images fibre and polymer is bright in these regions. These images were obtained with ion currents of $\sim 0.1 \text{ nA}$ giving a current density out of the 'static' SIMS regions. Nevertheless, it is clear that with fast data acquisition interface layers could be imaged using the approach described above. As composite materials involving organic polymers continue to make inroads into fields previously dominated by metal and alloys the requirement for this type of analysis must increase.

CONCLUSIONS

The major advantage of XPS for polymer surface and interface characterization is its ability to detect elements and give easily quantified data. Derivatization uses these factors to overcome limitations in functional group specificity of binding energy chemical shifts. Static SIMS has distinct advantages in terms of fingerprinting, imaging and microanalysis, and surface sensitivity. However, the combination of XPS and SIMS gives the best results. Instruments so set up can relatively easily perform ion scattering spectroscopy (ISS) which gives elemental information from the top atomic layer and hence completes a formidable trio of techniques.

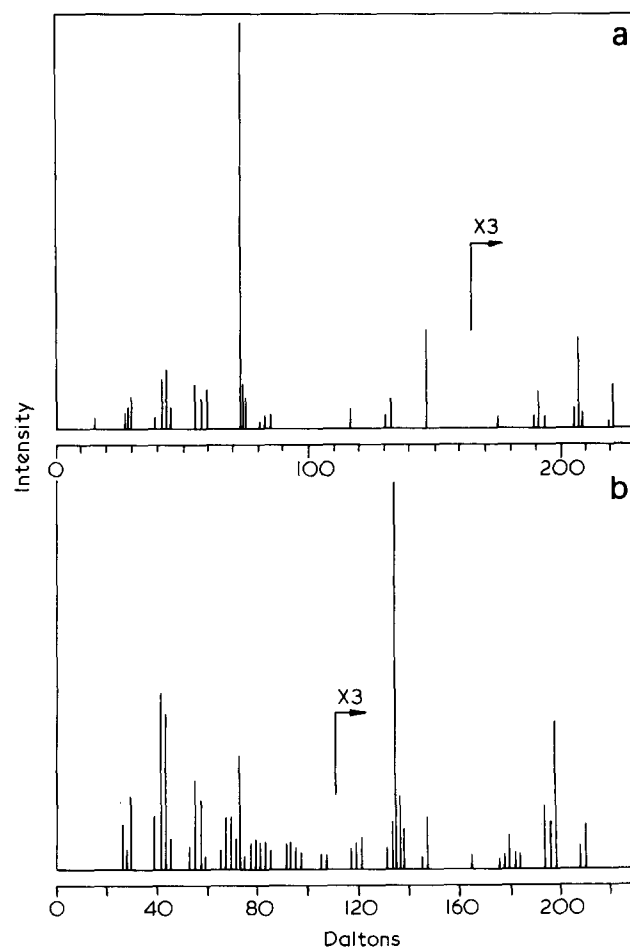


Figure 23 (a) Positive SIMS from large central spot of *Figure 21(a)*, $10^3 \text{ counts s}^{-1}$ f.s.d. (b) Positive SIMS from area corresponding to *Figure 22(c)*, $10^3 \text{ counts s}^{-1}$ f.s.d.

ACKNOWLEDGEMENT

It is a pleasure to acknowledge the contributions made to these developments by C. R. Kendall and A. B. Wootton. Thanks are also due to VG Scientific Ltd for the loan of equipment which made possible the SIMS imaging experiments.

REFERENCES

- 1 Clark, D. T. and Kilcast, D. *Nature* 1971, **233**, 77
- 2 Clark, D. T. in 'Photon, Electron and Ion Probes of Polymer Structure and Properties', Eds D. W. Dwight, T. J. Fabish, and H. R. Thomas', ACS Symposium Series 162, American Chemical Society (1981) and refs. therein
- 3 Briggs, D. 'Applications of XPS in Polymer Technology' in 'Practical Surface Analysis by Auger and X-ray Photoelectron Spectroscopy, Eds D. Briggs and M. P. Seah, Wiley, Chichester UK (1983)
- 4 von Brecht, H., Mayer, F. and Binder, H. *Makromol. Chem.* 1973, **33**, 89
- 5 Dwight, D. W. and Riggs, W. M. *J. Coll. Interface Sci.* 1974, **47**, 650
- 6 Hammond, J. S. Abstr. Chem. Soc. Nat. Meeting Div. Polym. Chem., Houston, **179** (1980)
- 7 Batich, C. D. and Wendt, R. C. in ref. 2
- 8 Everhart, D. S. and Reilley, C. N. *Anal. Chem.* 1981, **53**, 665
- 9 Everhart, D. S. and Reilley, C. N. *Surf. Interface Anal.* 1981, **3**, 126, 258
- 10 Briggs, D. and Kendall, C. R. *Polymer* 1979, **20**, 1053
- 11 Briggs, D. and Kendall, C. R. *Int. J. Adhesion Adhesives* 1982, **2**, 13
- 12 Reilley, C. N., Everhart, D. S. and Ho, F. F.-L. 'ESCA Analysis of Functional Groups on Modified Polymer Surfaces', in 'Applied Electron Spectroscopy for Chemical Analysis', Eds H. Windawi and F. F.-L. Ho, Wiley, New York (1982)
- 13 Briggs, D. 'Surface Treatments for Polyolefins' in 'Surface Analysis and Pretreatment of Plastics and Metals' Ed. D. M. Brewis, Applied Science, London (1982)
- 14 Owens, D. K. *J. Appl. Polym. Sci.* 1975, **19**, 265
- 15 Blythe, A. R., Briggs, D., Kendall, C. R., Rance, D. G. and Zichy, V. J. I. *Polymer* 1979, **19**, 1273
- 16 Brewis, D. M. and Briggs, D. *Polymer* 1981, **22**, 7
- 17 Gardella, J. A. and Hercules, D. M. *Anal. Chem.* 1980, **52**, 226
- 18 Gardella, J. A. and Hercules, D. M. *ibid* 1981, **53**, 1879
- 19 Briggs, D. and Wootton, A. B. *Surf. Interface Anal.* 1982, **4**, 109
- 20 Briggs, D. *ibid* 1982, **4**, 151
- 21 Briggs, D. *ibid* 1983, **5**, 113
- 22 Briggs, D. in 'Ion Formation from Organic Solids' Ed A. Benninghoven, Springer-Verlag, Berlin, p 156 (1983)
- 23 Briggs, D., Hearn, M. J. and Ratner, B. D. *Surf. Interface Anal.* 1984, **6**, 184
- 24 Briggs, D., Brown, A., van der Berg, J. and Vickerman, J. C. in 'Ion Formation from Organic Solids' Ed A. Benninghoven, Springer-Verlag, Berlin, p 156 (1983)
- 25 Bystry, F. A. and Penn, L. S. *Surf. Interface Anal.* 1983, **5**, 98
- 26 Yates, K. and West, R. H. *ibid* 1983, **5**, 217
- 27 Yates, K. and West, R. H. *ibid* 1983, **5**, 133
- 28 Paynter, R. W. *ibid* 1981, **3**, 186
- 29 Paynter, R. W., Ratner, B. D. and Thomas, H. R. *ACS Polym. Prepr.* 1983, **24**, 13
- 30 Biemann, K. in 'Mass Spectrometry: Organic Chemical Applications', McGraw Hill, New York (1962), p 171
- 31 Briggs, D. and Bayley, A. unpublished results

Note added in proof

More recent experiments indicate that the use of 2 keV Xe⁺ is optimum, giving higher yields of high mass clusters and lower rates of sample damage (Briggs, D. and Hearn, M. J. submitted to *Spectrochim. Acta.*).

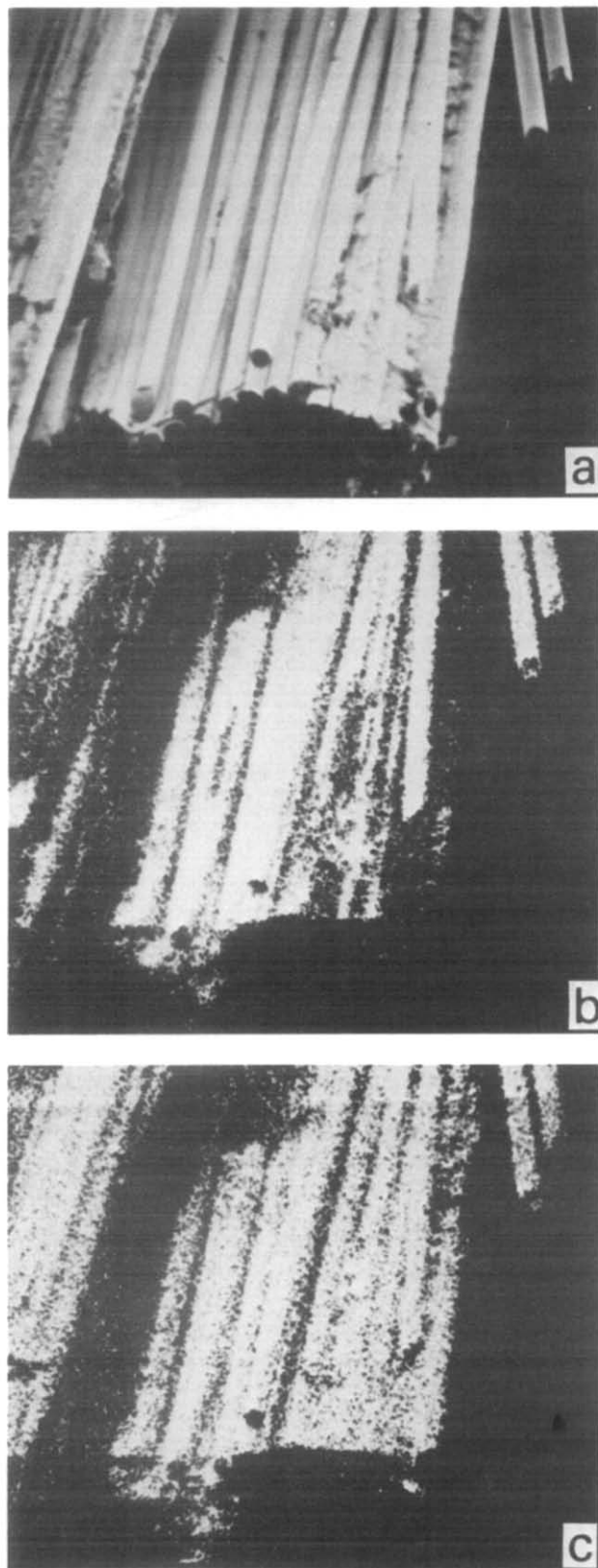


Figure 24 Images from carbon fibre/thermoplastic polymer composite fracture surface induced by Ga⁺ ions: (a) secondary electron image, (b) negative secondary ions of mass 26 (C₂H₂⁻), (c) negative secondary ions of mass 24 (C₂⁻). Scale is indicated by fibre diameter = 7 μm